IEEE Access
Multidisciplinary | Rapid Review | Open Access Journal

Received September 1, 2019, accepted September 14, 2019, date of publication September 17, 2019,
date of current version September 30, 2019.

Digital Object Identifier 10.1109/ACCESS.2019.2941992

A Physical-Layer Scheduling Approach in Large-Scale Cooperative Networks

FARHAN NAWAZ[1], SYED ALI HASSAN[1], (Senior Member, IEEE), ALI JAVED HASHMI[1], AND HAEJOON JUNG[2], (Member, IEEE)

[1]School of Electrical Engineering and Computer Science (SEECS), National University of Sciences & Technology (NUST), Islamabad 44000, Pakistan
[2]Department of Information and Telecommunication Engineering, Incheon National University, Incheon 22012, South Korea

Corresponding author: Haejoon Jung (haejoonjung@inu.ac.kr)

The work of H. Jung was supported by the Incheon National University Research Grant in 2019.

ABSTRACT In a sensor, mesh, or ad hoc network, different transmissions take place between multiple source-destination pairs, which is referred to as *data flows*. In this paper, each data flow is associated with a certain duty cycle schedule to avoid collisions of multiple flows in an energy-efficient manner. Cooperative routes in the network are assumed to be linear and strip-shaped, where each hop or a level contains multiple nodes, and the distance between the nodes is kept constant. We assume all nodes in a cooperative route, which corresponds to one source-destination pair, follow the same duty cycle schedule, while schedules of different routes are orthogonal in time to avoid interference between routes. Therefore, when a new route is formed, it is important to select a duty cycle schedule that is not already in use by the nodes participating in the new route. As part of route set-up, an orthogonal frequency division multiplexing packet travels from the source to the destination, identifying the schedules in use by the nodes along the path. Our objective in this paper is to analyze the probabilities of detection for this method of detecting schedules, which is useful to gain insights into duty cycling-based medium access protocol design in the presence of multiple data flows. To this end, the successive transmissions in a linear network are modeled using an irreducible discrete time Markov chain. Also, three different approaches to detect a certain schedule are investigated, which are distinguished by the binary integration process with multiple sub-carriers corresponding to the schedule. We derive the probability transition matrix for the Markov chain based on different distributions of the received signal energy, the left eigenvector of which yields the probability of detection.

INDEX TERMS Wireless network, stochastic modeling, cooperative communication, Markov chains, scheduling.

I. INTRODUCTION

Wireless ad hoc networks (WANETs) have drawn renewed interest in the context of Internet-of-Things (IoT) networks, which supports ubiquitous information exchange and content sharing among various devices with minimum human intervention [1]. In WANETs for IoT, which are inherently decentralized without relying on a pre-existing infrastructure, nodes are typically battery-powered and hardware-limited devices [2]. Thus, to reduce the average power consumption, such small devices employ duty cycling, where the nodes sleeps in a low-current mode most of the time [3]. In addition, because of the restricted transmission range, the nodes in WANETs cannot send messages directly to far-off destinations. Thus, to convey a message to a distant destination, multi-hop transmission is adopted. For example, using multi-hop routing protocols such as the ad hoc on-demand distance vector (AODV) and the dynamic source routing (DSR), a multi-hop route is constructed between a source and destination pair, where each hop is a single-input-single-output (SISO) link [4]. However, such conventional SISO-based multi-hop networks suffer from multi-path fading, which may result in low energy efficiency and high packet error rates. In this context, cooperative transmission (CT), where multiple nodes collaborate to transmit the same message, is an effective technique to mitigate the performance degradation caused by the multi-path fading [5]–[7].

The associate editor coordinating the review of this manuscript and approving it for publication was Celimuge Wu.

Opportunistic Large Array (OLA) is one type of CT, where groups of cooperative relays are formed without coordination, which can be exploited to a broad range of IoT applications such as smart cities, smart factories, healthcare, and intelligent transportation systems [8]. In particular, the group transmission in OLA produces a signal-to-noise-ratio (SNR) advantage through array and diversity gains, based on which various OLA-based broadcast and unicast schemes are proposed, as in [9], [10]. For instance, the OLA-based routing protocols such as OLA Routing On-Demand (OLAROAD) and OLA with primary route setup (OLA-PRISE) in are demonstrated to be fast, reliable, energy-efficient, and robust against mobility [10]. In particular, the authors in [13] maximized the throughput of multi-packet OLA transmissions within a single flow on an OLA-based cooperative route, which corresponds to multimedia file transfer scenarios, by adjusting packet insertion rate for the time-division multiple access (TDMA)-based medium access control (MAC) protocol.

However, as emphasized in [10] and [11], there has not been much progress on *multi-flow* MAC protocols for OLA-based routes to handle inter-flow interference, mainly due to the distributed nature of the OLA transmissions. For example, the authors in [12] proposed a MAC and routing enabled cross-layer CT protocol. However they assumed a single channel shared by the entire network, and did not consider duty cycling to increase the network lifetime. Furthermore, the proposed scheme in [12] was designed based on carrier sensing mechanism, which is not appropriate for OLA-based networks, since it requires a centralized controller (or cluster head) in each cooperative hop. A MAC algorithm that combines both duty cycling and CT called cooperative MAC was proposed in [11] for wireless sensor networks (WSNs). However, they also assumed carrier sensing since the centralized architecture can be readily realized by the gateway (or sink) in WSNs, which cannot be adopted to the OLA-based networks. In spite of difficulties in designing an efficient duty-cycled MAC protocol on the top of the distributed nature of OLA-based networks, it is essential to handle multiple flows in IoT applications with a large number of devices.

Motivated by this fact, in this paper we propose a novel method to schedule multiple flows from a physical layer perspective, which enables multiple OLA-based routes with duty cycling to coexist without collisions. To be specific, in the proposed scheme, we first perform, as part of OLA route setup, a multi-hop binary integration of each duty cycle schedule that is already occupied along the route, using a CT technique similar to the OLA and orthogonal frequency division multiplexing (OFDM) modulation. The binary integration, also known as M-out-of-N detection, is the combination of individual detections of an event to make a single aggregate detection of the event [15]–[17]. In this work, for the duty cycle coordination of multiple flows, binary integration is performed in each hop using the method of semi-cooperative spectral fusion (SCSF), which was proposed in [17] for one-hop networks. While similar to OLA, where a group of nodes transmit at the same time, SCSF allows the nodes to transmit different messages, each based on their individual detections, so that a receiver is able to estimate M and hence make a decision on the event. Applying this idea to the OLA-based multi-hop networks, in the proposed binary integration technique, independent SCSF-based decisions on multiple duty cycle schedules can be made in parallel using the OFDM waveforms.

The key contributions in this paper are four-fold. First, we propose a novel scheme to detect a duty cycle schedule available for a new OLA-based route, while the route is being constructed. Thus, right after the route setup procedure, the source node is able to select a duty cycle schedule for the newly constructed route that is orthogonal to all existing schedules in use by the nodes along the route. Second, we present an analytical framework for the multi-hop version of SCSF using OFDM, which is employed for the proposed scheme. Third, we analyze the probabilities of detection for three different approaches to process observations on multiple sub-carriers. Lastly, we present both simulation and numerical results to validate our analysis.

The rest of the paper is organized as follows. In Section II, we introduce previous studies that have similar objectives but differ substantially. Then, in Section III, we describe the system model. Also, multi-hop cooperative networks are analyzed by Markov chains in Section IV. In Section V, we formulate the probability transition matrix, which is the key information for performance analysis. In Section VI Numerical and simulation results are presented to investigate the impacts of various system parameters. Then, we conclude this paper in Section VII.

II. RELATED WORK

The problem addressed in this paper is similar to the traffic analysis in [18] and [19], where packet flow patterns in wireless sensor networks (WSNs) are estimated. However, they used an *offline* algorithm for the detection of the information flows by using timing analysis, which can incurs excessive latency especially in large-scale networks. On the other hand, a real-time scheduling was proposed in [20] for event-triggered and time-triggered flows in the industrial WSNs. However, their proposed scheme requires the centralized network architecture, which is not desirable for the WANETs. Furthermore, the authors in [21] presented a method of coverage optimization for sensor scheduling in duty-cycled WSNs using a virtual hexagon partition composed of hexagonal cells. However, they assumed that the nodes are aware of their locations, which requires the Global Positioning System (GPS) or other positioning systems in practice. Also, in [22], a distributed link scheduling (DLS) protocol is proposed for WSNs based on graph coloring. However, the CT-based routes with extended transmission ranges cannot be interpreted by their graph theory-based approach. Moreover, the authors in [23] investigated centralized scheduling strategies for cooperative networks, which is not applicable

to decentralized WANETs. Also, while carrier sensing-based schemes with cluster heads were assumed as in [11] and [12], there has not been any detailed scheduling or duty-cycle allocation algorithm to avoid inter-flow interference with the de-centralized architecture.

Different from these existing works, in this paper, we tackle the multi-flow scheduling problem by multi-hop binary integration for CT-based WANETs in a fully distributed fashion. Furthermore, this work is unique in the sense that duty-cycle scheduling is performed as part of route construction, which can be employed to MAC protocols to coordinate multiple strip-shaped OLA-based routes. In other words, we consider the problem of detecting multiple schedules running in a network in the presence of multiple source-destination pairs. Excessive collisions may arise when all the pairs want to communicate with each other at the same time. Also, some intermediate nodes that belong to one source-destination path can also be parts of another path. Therefore, to avoid inter-flow interference among different paths, each path must have a unique schedule, and all the transmissions take place according to the schedules assigned. In duty-cycled networks, these schedules must be time multiplexed in such a way that when one path is transmitting, the other paths go in a silent mode. Thus, every time when a new source-destination pair wants to communicate with each other, it first identify the pre-exsiting schedules along the constructed route, and then starts its transmission in a schedule, which is not used by intersecting routes.

III. SYSTEM MODEL

We consider a large-scale cooperative network, in which multiple source-destination pairs exist and multi-hop routes have been formed between each source-destination pair. In contrast to the conventional SISO-based multi-hop networks, OLA-based networks can guarantee scalability even with extremely high node density [8]. Thus, in practice, the large-scale cooperative networks can be used in IoT-based smart environments (e.g., smart homes, smart cities, smart transportation, smart industry, and smart building environments), where infinitely large number of device and sensors are interconnected [24].

We assume a deterministic node placement strategy such that a two-dimensional linear network is formed for each route as shown in Figure 1. This implies that for each route, multiple nodes are present in each hop, constituting a virtual multiple-input multiple-output (MIMO) multi-hop scenario. We now assume that a new source-destination pair appears in the network, in the horizontal route, which happens to cross one or more already established paths. For instance, in Figure 1, the new route crosses two established routes represented by two vertical paths. We define ''intersection nodes'' to be nodes that are common to both the new route and an intersecting route. In Figure 1, there are two sets of intersection nodes, each set having four nodes. The destination node is located m hops away from the source node. We assume that in this new source-destination path, an

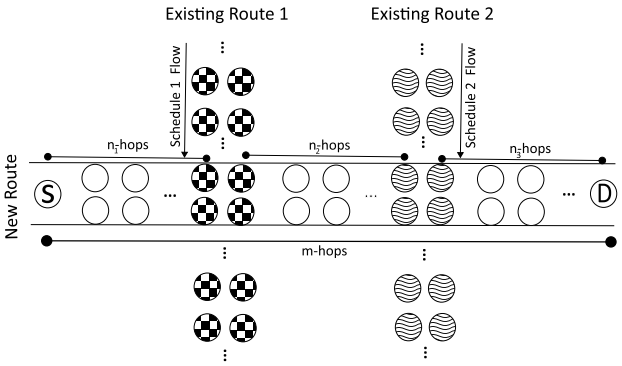

FIGURE 1. The system model showing a new source-destination route crossing two already existing routes. There are 4 nodes in each hop.

existing intersecting route is present after every n_i hops, where i is an integer. Hence n_i can be defined as the number of hops from the previous intersecting route $i-1$ to current intersecting route i. Furthermore, $i=1$ indicates the number of hops from the source node to the first intersecting route. Each intersecting route follows a certain schedule $s \in \boldsymbol{S}$ from the set $\boldsymbol{S} = \{1, 2, \ldots, S\}$, where S is the total number of schedules that the network can have at one time.

Recall that our objective in this paper is to assign an orthogonal schedule to this new route so that the nodes sleep and wake in such a manner that there is no interference on them from other routes. In the example given in Figure 1, the new route should follow any schedule other than $\{1, 2\}$, because they are currently in use. The source in this case initiates a polling query, which travels all the way to the new destination. The purpose of this polling query is to learn the schedules of the intersecting routes. When the intersection nodes, which are present in this new path, receive this polling query, they insert the information of the schedules that they follow. The destination node when receives this query packet, detects the schedules that are already occupied in the network. In reply to this polling query, the destination node assigns a new schedule (that is not in use) to its corresponding source by propagating a message in the backward direction towards the source on the already established route. Through this message, the intermediate nodes also know their schedule for this new path.

For the detection of existing schedules at the new destination node, we consider our source packet to be consistent with an OFDM symbol. The total number of orthogonal sub-carriers in an OFDM packet are KS, where $K \in \boldsymbol{Z}^+$, i.e., a positive integer. These sub-carriers are partitioned into S bands in such a way that for each Schedule i, there is a corresponding band B_i. Each band contains K sub-carriers, which are used to report the information of one particular schedule. In Figure 1, we suppose that the total number of schedules present in the network are 4, i.e., $S=4$. The OFDM packet in this case contains 4 bands as shown in Figure 2. Let the number of sub-carriers K, assigned to each band be 3. The overall packet, therefore, consists of 12 sub-carriers. Here, the band B_1 is reserved for Schedule 1, B_2 for Schedule 2,

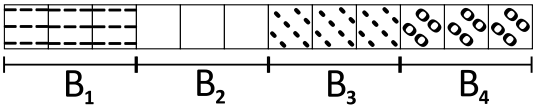

FIGURE 2. The OFDM packet with 12 sub-carriers, i.e., $S = 4$ and $K = 3$.

and so on. If the source is an intersection node, it initiates the polling process by transmitting an on-off keying (OOK) symbol "1" in each sub-carrier of the band corresponding to the schedule in use by its intersecting route. When each node in the first hop receives this packet, it employs energy detection to detect the presence/absence of symbols in each sub-carrier of the received OFDM packet. If energy in a band representing a certain schedule, is detected correctly, then that schedule is detected successfully. When relaying, a node that has detected a schedule will transmit a symbol "1" in each sub-carrier corresponding to the detected schedule. Incorrect decoding of the symbols can cause misses and false alarms in the network. In a false alarm, a schedule that is absent in the network, appears to be detected. When an intersection node that follows a schedule s receives this OFDM packet, it performs energy detection in each sub-carrier and inserts an OOK symbol 1 in all the sub-carriers corresponding to Band B_s. On the other hand, in rest of the bands, the node regenerates the previous information obtained after performing energy detection. For the case discussed in Figure 1 and Figure 2, when the node that follows Schedule 1 receives an OFDM packet, it inserts its schedule information by transmitting OOK symbol 1 in all the sub-carriers of B_1 band and in the rest of the bands, the previous information propagates, as obtained through energy detection. Similarly, when the node following Schedule 2 receives this packet, it transmits OOK symbol 1 in all the sub-carriers of B_2 band, and propagates the previous information in rest of the bands. The destination node when receives this packet, detects that the Schedule 1 and 2 are already occupied in the network. Hence, it assigns an orthogonal schedule such as 3 or 4 to the source node. If, because of the false alarms, Schedule 3 is also detected at the destination, then the destination node informs the source node to follow Schedule 4.

We assume that all the nodes transmit the message with the same transmit power, P_t, per sub-carrier, defined as $P_t = \frac{P}{KS}$, where P represents the total power of an OFDM packet. Here all channels are assumed to be Rayleigh fading. The message travels all the way to the destination through multiple hops. For a node in a Level l, the signal received at any sub-carrier j of the OFDM packet is given by

$$y_j = G_j + n_j, \tag{1}$$

where G_j is the sum of complex channel gains from the N decode-and-forward (DF) nodes present in the previous level or hop, such that G_j is a complex Gaussian random variable i.e., $G_j \sim \mathcal{CN}(0, NP_t)$. Similarly, $n_j \sim \mathcal{CN}(0, \sigma_n^2)$ is the noise in jth sub-carrier with variance σ_n^2. The energy in a sub-carrier j is thus exponentially distributed, i.e., $|y_j|^2 \sim \exp(\lambda)$, where $\lambda = NP_t + \sigma_n^2$, with the probability distribution function (PDF) given by

$$f_{|y_j|^2}(y) = \frac{1}{\lambda} \exp\left(\frac{-y}{\lambda}\right). \tag{2}$$

We note that the proposed scheme is suitable for the networks with hardware-limited nodes such as small sensors, because we use a simple energy detection scheme can be applied to OOK signals, resulting in the practical implementation of lowest achievable complexity [25]. Further, the proposed scheme can be executed in a fully distributed manner without requiring any infrastructure or centralized controller (or cluster head).

IV. MODELING BY MARKOV CHAIN

At any level l, since the total number of schedules present in a network are S, so the total possible packet states are 2^S. The OFDM packet received by a node can be in any of the possible states depending upon the schedules detected. The packet states are defined as

$$\mathbb{Y}(l) = [\mathbb{X}_1(l), \mathbb{X}_2(l), \ldots, \mathbb{X}_S(l)], \tag{3}$$

where $\mathbb{X}_i(l)$ is the binary indicator random variable for ith schedule at Level l, given by

$$\mathbb{X}_i(l) = \begin{cases} 1 & \text{if } i\text{th schedule is detected} \\ 0 & \text{if } i\text{th schedule is not detected} \end{cases} \tag{4}$$

The detection of each schedule, i.e., the value of $\mathbb{X}_i(l)$ itself depends on the detection of the received signal energy in each of the K sub-carriers, assigned to that schedule. We follow three different cases as described here to get the value of $\mathbb{X}_i(l)$.

A. STRICT APPROACH

In this approach, Schedule s is detected only when the received signal energy in each of the K sub-carriers in Band B_s is greater than a certain energy threshold τ. If the received energy in any of the K sub-carriers is less than τ, then the schedule is assumed to be not detected. Here, we assume that all the signals in one sub-carrier are i.i.d complex Gaussian with the zero mean. The probability of detection of sub-carrier, j, is given by

$$\mathbb{P}_d = \mathbb{P}\{|y_j|^2 > \tau\}, \quad \forall j \in \{1, 2, \ldots, K\}, \quad K \in B_s. \tag{5}$$

Thus, for the strict case, the probability of detection of one schedule, s, is defined as

$$\mathbb{P}_s^{(s)} = \prod_{j=1}^{K} \mathbb{P}\{|y_j|^2 > \tau\}, \quad K \in B_s, \tag{6}$$

$$\mathbb{P}_m^{(s)} = 1 - \prod_{j=1}^{K} \mathbb{P}\{|y_j|^2 > \tau\}, \quad K \in B_s, \tag{7}$$

where $\mathbb{P}_s^{(s)}$ and $\mathbb{P}_m^{(s)}$ denote the probability of successful detection and probability of miss, respectively, of the Schedule s.

B. LENIENT APPROACH

In the second method called the lenient approach, Schedule s is detected when the received signal energy in any of the K sub-carriers in Band B_s is greater than the threshold τ. The schedule is not detected only in that case, when the received signal energy in all of the K sub-carriers is less than τ. The probability of successful detection, $\mathbb{P}_s^{(s)}$, and probability of miss, $\mathbb{P}_m^{(s)}$, of the schedule s is expressed as

$$\mathbb{P}_s^{(s)} = 1 - \left(\prod_{j=1}^{K} \left(1 - \mathbb{P}\{|y_j|^2 > \tau\} \right) \right), \quad K \in B_s, \quad (8)$$

$$\mathbb{P}_m^{(s)} = \prod_{j=1}^{K} \left(1 - \mathbb{P}\{|y_j|^2 > \tau\} \right), \quad K \in B_s. \quad (9)$$

C. DIVERSITY APPROACH

In the diversity approach, Schedule s is detected if the combined received signal energy of all the K sub-carriers in Band B_s is greater than the threshold τ. The probability of successful detection, $\mathbb{P}_s^{(s)}$ and probability of miss, $\mathbb{P}_m^{(s)}$ of the Schedule s is given by

$$\mathbb{P}_s^{(s)} = \mathbb{P}\left\{ \sum_{j=1}^{K} |y_j|^2 > \tau \right\}, \quad K \in B_s, \quad (10)$$

$$\mathbb{P}_m^{(s)} = 1 - \mathbb{P}\left\{ \sum_{j=1}^{K} |y_j|^2 > \tau \right\}, \quad K \in B_s. \quad (11)$$

From (3), we can see that the outcomes of $\mathbb{Y}(l)$ are S-bit binary words, each constituting a state. These states in decimal form are written as $\{0, 1, \ldots, 2^S - 1\}$. Let b_l be the outcome of $\mathbb{Y}(l)$ at level l. For example, $b_l = 1010$ in binary indicates 10 in decimal, which implies that the node has detected Schedules 1 and 3 in this case. Therefore, $\mathbb{Y}(l)$ can be modeled as a discrete time finite state Markov Process with $\mathbb{P}$ as a probability measure, given by

$$\mathbb{P}\{\mathbb{Y}(l) = b_l | \mathbb{Y}(l-1) = b_{l-1}, \ldots, \mathbb{Y}(1) = b_1\} = \mathbb{P}\{\mathbb{Y}(l) = b_l | \mathbb{Y}(l-1) = b_{l-1}\}. \quad (12)$$

The packets can go from one transient state to any other transient state, therefore all of the packet states make an irreducible state space as shown in Figure 3. The Markov chain is defined by the probability transition matrix $\mathbf{P}$ of order $(2^S \times 2^S)$, which is defined on the corresponding states in $\mathbb{Y}$. The sum of each row of $\mathbf{P}$ is equal to 1. From the theory of Markov chains [26], a distribution $\boldsymbol{\pi} = (\pi_i, i \in \{1, 2, \ldots, 2^S\})$ is called υ-invariant distribution if $\boldsymbol{\pi}$ is the left eigenvector of the transition matrix $\mathbf{P}$ corresponding to the eigenvalue υ, i.e,

$$\boldsymbol{\pi}\mathbf{P} = \upsilon\boldsymbol{\pi}. \quad (13)$$

If $\upsilon = 1$, $\boldsymbol{\pi}$ is the stationary distribution. The distribution $\boldsymbol{\pi}$ is a row vector of size (1×2^S), with the entry π_i corresponding to the probability of occurrence of the State i. Our interest here is to find the distribution $\boldsymbol{\pi}$ of the transient states at each hop. Considering our system model, the distribution $\boldsymbol{\pi}$ at the nth hop can be determined as

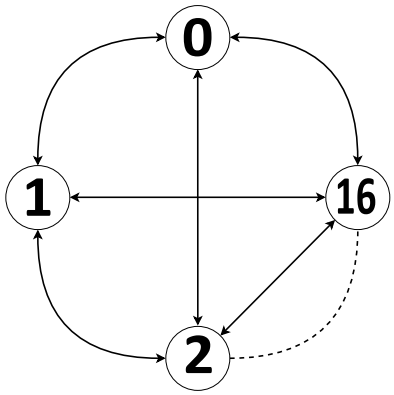

FIGURE 3. The state space representation of $\mathbb{Y}(l)$ for $S = 4$.

$$\boldsymbol{\pi}^{(n)} = \boldsymbol{\pi}^{(0)}\mathbf{P}^{(n)}, \quad (14)$$

where $\boldsymbol{\pi}^{(0)}$ is the initial distribution of the source packet. Here, we assume the source node does not follow any schedule, therefore, initially the source packet would be in state 0. This is because the source forwards the OFDM packet with all the sub-carriers filled with OOK symbol 0. Considering the example discussed in Figure 1 and Figure 2, the state of the packet at the source node is $\mathbb{Y}(0) = [0000]$. Hence, the initial distribution $\boldsymbol{\pi}^{(0)}$ in this case is a row vector of size (1×16) whose first entry is 1 and all other entries are zero represented as $\boldsymbol{\pi}^{(0)} = [1\ 0\ 0\ 0\ 0\ 0\ 0\ 0\ 0\ 0\ 0\ 0\ 0\ 0\ 0\ 0]$. If a node on the nth hop follows a certain schedule s for a pre-existing flow, then it updates the schedule information on the packet (i.e., inserts OOK symbol 1 in each of the K sub-carriers in Band B_s of the previously received OFDM packet). The distribution $\boldsymbol{\pi}^{(n)}$ then modifies to $\hat{\boldsymbol{\pi}}^{(n)}$ according to Algorithm 1. This distribution $\hat{\boldsymbol{\pi}}^{(n)}$ then becomes the initial distribution for finding $\boldsymbol{\pi}^{(n+1)}$. The distribution at the $(n+1)$th hop can then be determined as

$$\boldsymbol{\pi}^{(n+1)} = \hat{\boldsymbol{\pi}}^{(n)}\mathbf{P}. \quad (15)$$

Thus the packet travels all the way to the destination, which is m hops from the source. We find the distribution $\boldsymbol{\pi}^{(m)}$ at the destination, which gives the information about the occurrence of each schedule in the network.

How Algorithm 1 works can be explained by an example scenario as follows. Suppose that a node located at the nth hop follows Schedule 2, i.e,. $s = 2$, and the total number of schedules present in the network are $S = 4$. The distribution vector $\boldsymbol{\pi}^{(n)}$ obtained at the nth hop is shown at the top in Figure 4. The algorithm defines two sets $\boldsymbol{A}$ and $\boldsymbol{B}$, the sizes of which are $(1 \times 2^{S-1})$. The value of δ is calculated by $\delta = 2^{(S-s)}$, which corresponds to $2^{(4-2)} = 4$ in this example. Depending on the value of δ, the algorithm picks first δ (i.e., 4 in this example) values from $\boldsymbol{\pi}^{(n)}$ vector and places them into set $\boldsymbol{A}$, and the next δ values in set $\boldsymbol{B}$. This process continues until the sets $\boldsymbol{A}$ and $\boldsymbol{B}$ are filled as shown in Figure 4. These two sets $\boldsymbol{A}$

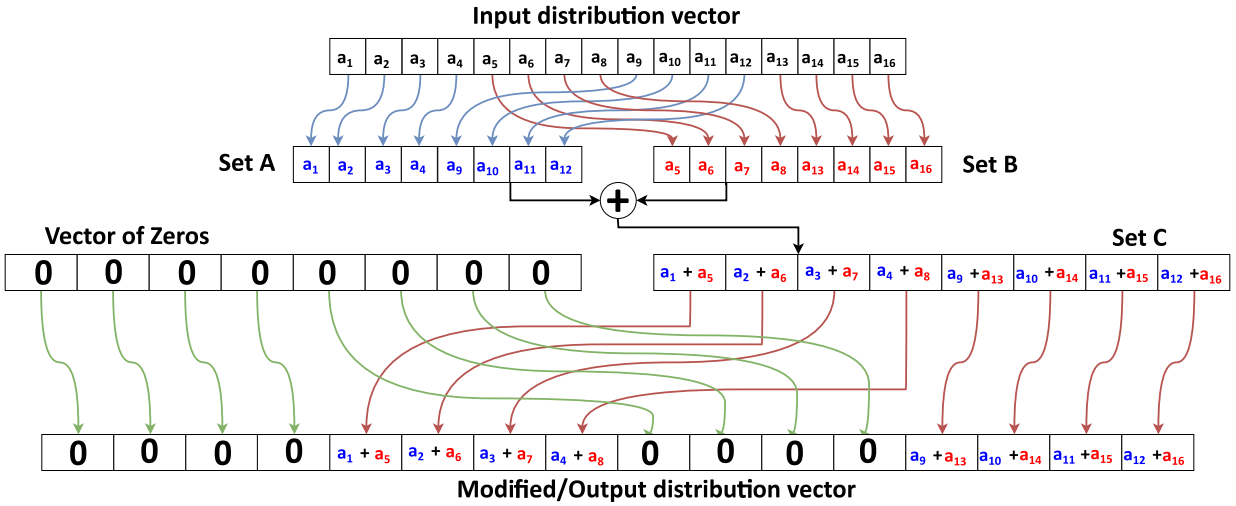

FIGURE 4. The working of Algorithm 1 for $S = 4$, $s = 2$, and $\delta = 4$.

Algorithm 1 Finding Initial Distribution

Input : $\boldsymbol{\pi}^{(n)}$
Output: $\hat{\boldsymbol{\pi}}^{(n)}$
initialization: $i \leftarrow 1, j \leftarrow 1, a \leftarrow 1, b \leftarrow 1$;
$\boldsymbol{S} \leftarrow \{1, 2, \ldots, S\}$, a set of all schedules;
$s \in \boldsymbol{S}$, s is the node schedule;
$\boldsymbol{O}$, a zero vector with the same size as $\boldsymbol{S}$;
$\delta := 2^{S-s}$, find value;
while $i \leq 2^S$ **do**
  $\boldsymbol{A}[a : \delta + a - 1] := \boldsymbol{\pi}^{(n)}[i : \delta + i - 1]$;
  $\boldsymbol{B}[a : \delta + a - 1] := \boldsymbol{\pi}^{(n)}[\delta + i : 2\delta + i - 1]$;
  $i := 2\delta + i$;
  $a := \delta + a$;
end
$\boldsymbol{C} = \boldsymbol{A} + \boldsymbol{B}$;
while $j \leq 2^{S-1}$ **do**
  $\hat{\boldsymbol{\pi}}^{(n)}[b : 2\delta + b - 1] := \Big[\boldsymbol{O}[j : j + \delta - 1]$
  $\boldsymbol{C}[j : j + \delta - 1]\Big]$;
  $j := \delta + j$;
  $b := 2\delta + b$;
end

and $\boldsymbol{B}$ are added to make the third set $\boldsymbol{C}$. Then, a zero vector, which has the same size as the set $\boldsymbol{C}$, is initialized. The modified distribution vector $\hat{\boldsymbol{\pi}}^{(n)}$ is obtained by placing the first δ values from the zero vector and the next δ values from the set $\boldsymbol{C}$ into $\hat{\boldsymbol{\pi}}^{(n)}$ vector. The same repeats for the other values until the distribution vector completes. The reason for using this Algorithm is due to the fact that when a node receives an OFDM packet, it inserts its schedule information into the packet. Because of this, the previous information inside the packet changes, by which the initial distribution also varies. In order to model a Markov chain, the initial distribution is to be determined at the node for finding the state distribution at the next level.

It must be noted that if a node follows more than one schedule, i.e., $s = 2$ and 3, the modified distribution vector can be obtained by following the Algorithm 1 twice. For the first time, we find $\tilde{\boldsymbol{\pi}}^{(n)}$ for $s = 2$, then for the second time, find $\hat{\boldsymbol{\pi}}^{(n)}$ for $s = 3$ using the same $\tilde{\boldsymbol{\pi}}^{(n)}$ obtained in the previous case ($s = 2$), as the input distribution in the Algorithm 1. This $\hat{\boldsymbol{\pi}}^{(n)}$ serves as the initial distribution for finding $\boldsymbol{\pi}^{(n+1)}$ in this case.

V. FORMULATION OF THE TRANSITION PROBABILITY MATRIX

The state transition matrix $\mathbf{P}$ is derived in this section for our system model. The state distribution of a packet can easily be obtained by finding the left eigenvector of the $\mathbf{P}$ matrix. Let we assume i and j as a pair representing the states of a packet such that $i, j \in \{0, 1, 2, \ldots, 2^S - 1\}$. These states i and j in a S-bit binary word can be written as $i = (\beta_{S-1}^{(i)}, \ldots, \beta_1^{(i)}, \beta_0^{(i)})$ and $j = (\beta_{S-1}^{(j)}, \ldots, \beta_1^{(j)}, \beta_0^{(j)})$, respectively. Since, the probability of detection and the probability of miss of every schedule in an OFDM packet can be represented using the same mathematical expression, i.e., $\mathbb{P}_s^{(1)} = \mathbb{P}_s^{(2)} =, \ldots, = \mathbb{P}_s^{(s)} = \mathbb{P}_s$ and $\mathbb{P}_m^{(1)} = \mathbb{P}_m^{(2)} =, \ldots, = \mathbb{P}_m^{(s)} = \mathbb{P}_m$, so, the probability of transition $\mathbf{p}_{ij}$ from state i to state j is given by

$$\mathbf{p}_{ij} = \prod_{z} (\mathbb{P}_m) \cdot \prod_{S-z} (\mathbb{P}_s) \,, \tag{16}$$

where $z = \sum_{k=0}^{S-1} \left(\beta_k^{(i)} \oplus \beta_k^{(j)}\right)$. From (5), the probability of detection of one sub-carrier, j, is defined as

$$\mathbb{P}_d = \mathbb{P}\{|y_j|^2 > \tau\} = \int_{\tau}^{\infty} f_{|y_j|^2}(y) dy, \tag{17}$$

where τ is the energy threshold. Simplifying the above equation gives

$$\mathbb{P}_d = \exp\left(-\frac{\tau}{\lambda}\right). \tag{18}$$

The state transition matrix **P**, for all the three approaches, is found in the following three cases.

A. TRANSITION PROBABILITY OF STRICT APPROACH

From (6), the probability of successfully detecting a schedule is given by

$$\mathbb{P}_s = (\mathbb{P}_d)^K = \exp\left(-\frac{\tau K}{\lambda}\right), \tag{19}$$

where $\lambda = N_j P_t + \sigma_n^2$. The probability of miss in this case is found using (7) as

$$\mathbb{P}_m = 1 - (\mathbb{P}_d)^K = 1 - \exp\left(-\frac{\tau K}{\lambda}\right). \tag{20}$$

Also, the probability of transition $\mathbf{p}_{ij}$ from state i to state j from (16), can be written as

$$\mathbf{p}_{ij} = \prod_{z}\left(\exp\left(-\frac{\tau K}{\lambda}\right)\right) \cdot \prod_{S-z}\left(1 - \exp\left(-\frac{\tau K}{\lambda}\right)\right). \tag{21}$$

B. TRANSITION PROBABILITY OF LENIENT APPROACH

From (8), the probability of successfully detecting a schedule is given by

$$\mathbb{P}_s = 1 - (1 - \mathbb{P}_d)^K = 1 - \left(1 - \exp\left(-\frac{\tau}{\lambda}\right)\right)^K. \tag{22}$$

The probability of miss using (9) is expressed as

$$\mathbb{P}_m = (1 - \mathbb{P}_d)^K = \left(1 - \exp\left(-\frac{\tau}{\lambda}\right)\right)^K. \tag{23}$$

From (16), the state transition probability $\mathbf{p}_{ij}$ can be expressed as

$$\mathbf{p}_{ij} = \prod_{z}\left(1 - \left(1 - \exp\left(-\frac{\tau}{\lambda}\right)\right)^K\right) \cdot \prod_{S-z}\left(\left(1 - \exp\left(-\frac{\tau}{\lambda}\right)\right)^K\right). \tag{24}$$

C. TRANSITION PROBABILITY OF DIVERSITY APPROACH

In this approach, the combined energy of all the K sub-carriers is to be determined. The distribution of which is obtained by summing the K exponential RV's with identical mean λ, which is defined as $Gamma(K, \lambda)$ [27]. Here K and λ represent the shape and scale parameters of the Gamma function, respectively. Now, from (10), the probability of successfully detecting a schedule in this case is given by

$$\mathbb{P}_s = \sum_{p=0}^{K-1} \frac{1}{p!}\left(\frac{\tau}{\lambda}\right)^p \exp\left(-\frac{\tau}{\lambda}\right), \tag{25}$$

while the probability of miss of schedule, using (11), can be represented as

$$\mathbb{P}_m = 1 - \left(\sum_{p=0}^{K-1} \frac{1}{p!}\left(\frac{\tau}{\lambda}\right)^p \exp\left(-\frac{\tau}{\lambda}\right)\right), \tag{26}$$

TABLE 1. Simulation parameters.

Parameter	Value
Monte Carlo trials in simulation	10^5
number of nodes in each hop N	4
transmit power P	10 dB
noise variance σ_n^2	1
energy threshold τ	0.5
total number of schedules S	4
number of sub-carriers per schedule K	3
end-to-end hop count m	30
hop counts n_1, n_2, n_3 in Figure 1	10

The probability of transition $\mathbf{p}_{ij}$ from state i to state j from (16), can therefore be written as

$$\mathbf{p}_{ij} = \prod_{z}\left(\sum_{p=0}^{K-1} \frac{1}{p!}\left(\frac{\tau}{\lambda}\right)^p \exp\left(-\frac{\tau}{\lambda}\right)\right) \cdot \prod_{S-z}\left(1 - \left(\sum_{p=0}^{K-1} \frac{1}{p!}\left(\frac{\tau}{\lambda}\right)^p \exp\left(-\frac{\tau}{\lambda}\right)\right)\right). \tag{27}$$

VI. NUMERICAL RESULTS AND DISCUSSION

In this section, we present numerical and the simulation results to validate our analysis in the previous section. At the same time, we will investigate the impacts of with various system parameters to better evaluate the proposed scheme. The simulation results are obtained through 10^5 random trials. The parameters both for numerical calculation and simulation are given in Table 1, unless specified otherwise. Also, we note that the simulation parameters are chosen to reflect practical large-scale networks, based on the values used in [10], [13].

In Figure 5, the probability of the packet to be in state $Y(l) = \{1100\}$ is shown, where the horizontal axis corresponds to the number of hops from the source to the destination (i.e., the end-to-end hop count). Also, the four blue curves indicate the numerical results with the different transmit powers of the OFDM packet (i.e., $P = \{5, 8, 10, 12\}$ dB), while the red squares represent the corresponding simulation results. As shown in the figure, we first observe that the analytical results of the state probabilities obtained using the Markov chain show the excellent correlation with the simulation results, which validates our analysis. Moreover, the state probability decreases, as the end-to-end hop count increases. In addition, as the transmit power P increases, the state probability also increases.

Figure 6 shows how the probability of detection changes, as the transmit power P increases. Also, we compare the three different approaches analyzed in Section V with the different numbers of sub-carriers per schedule $K = \{1, 2, 3\}$. We assume that multiple flows in the network are organized with 4 schedules (i.e., $S = 4$), where Schedules 1 and 2 are already occupied by other source-destination paths. We assume that the destination node is 30 hops away from the source node (i.e., $m = 30$). The nodes that follow

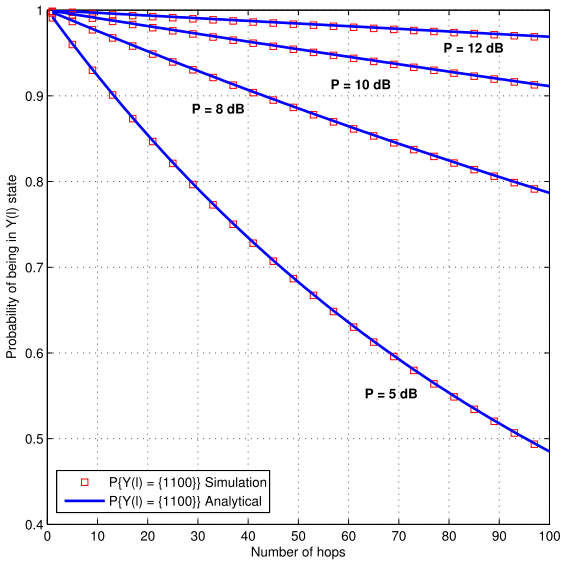

FIGURE 5. The probability of detection for different number of hops for varying P.

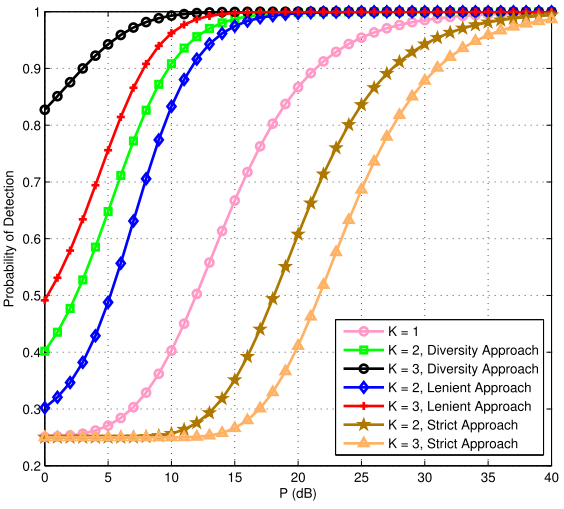

FIGURE 6. The probability of detection against the transmit power, P, for varying K.

Schedules 1 and 2 are 10 and 20 hops away from the source node, respectively (i.e., $n_1 = n_2 = n_3 = 10$ in Figure 1). First of all, we can observe the numerical results are in line with the simulation results, which verifies our analysis. Also, we observe that, for the lenient and diversity approaches, the probability of detecting both the schedules at the destination increases, when the number of sub-carriers, K assigned to each schedule increases. The reason is that, for the lenient, when K increases, the probability of successfully detecting any sub-carrier out of K sub-carriers increases, as noted in (8). Similarly, the diversity approach can benefit from the increased number of independent observations from different sub-carriers (i.e., diversity channels), as derived in (10). In contrast, in the strict approach, as K increases, the probability of successful detection of all the sub-carriers at a time decreases, which can be explained by (6). Also, for the special

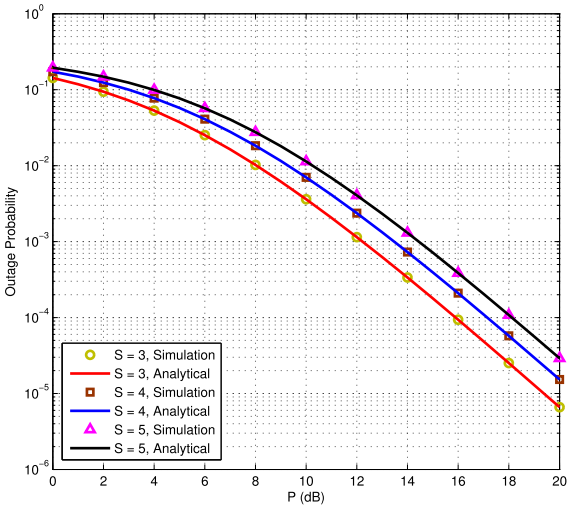

FIGURE 7. The probability of miss vs. the transmit power, P, for varying S.

case of $K = 1$, which can be regarded as the conventional single channel detection without duty cycling [10], all the approaches provide the same performance, because there is no distinction among them.

Figure 7 shows the outage probability (or the probability of miss) of the diversity approach under the variation of the transmit power P, which correspond to the vertical and horizontal axes, respectively. We assume the same parameters as in Figure 6, except that different number of schedules are used (i.e., $S = \{3, 4, 5\}$) to investigate the impact of S. Also, the number of sub-carriers per schedule is set to be three (i.e., $K = 3$). In the figure, as the total number of schedules in the network S increases, the outage probability also increases. This is due to the fact that the transmit power of each sub-carrier decreases, when we increase the number of schedules in a network. In other words, when S increases, the bands in an OFDM packet also increase in order to accommodate more schedules. Therefore, the total power of an OFDM packet is divided by the term KS, which implies that each sub-carrier gets a fraction of $1/KS$ of the total OFDM packet power. Also, the analytical results shows the almost perfect match with the simulation results, which validates our analysis.

To consider different placements of the multiple flows in the cooperative route, different hop combinations (i.e., different values of n_1, n_2 and n_3) are tested in Figure 8. The y-axis indicates the probability of detection of the diversity approach, while the x-axis corresponds to the hop combinations. We note that the probability of detection is obtained with the same end-to-end hop count m of 60 for all the combinations. Also, we assume $S = 4$ and $K = 3$, respectively. The total transmit power P of the OFDM packet is set to be 10 dB. In the figure, for every combination of n_1, n_2 and n_3, the gray and blue bars indicate the probabilities of detection of Schedules 1 and 2, respectively, while the red and peach bars represent the probabilities of false alarm for Schedules 3 and 4, respectively. In the figure, in all of the four cases, the probability of detection of Schedule 2 is higher than that of Schedule 1. This is because the node that

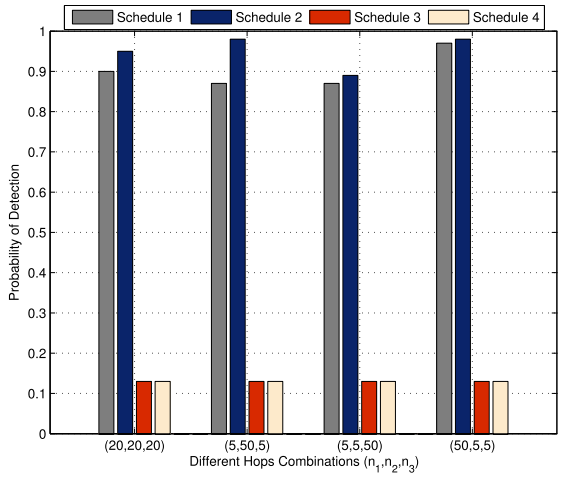

FIGURE 8. The probability of detection for different combinations of n_1, n_2 and n_3.

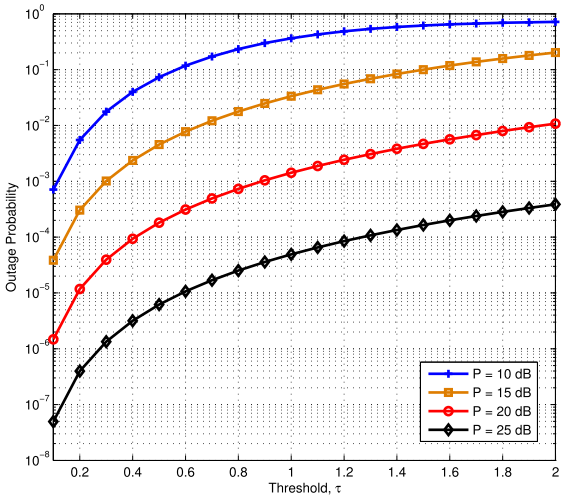

FIGURE 9. The probability of outage versus different thresholds τ with $S = 4$.

follows Schedule 2 is closer to the destination compared to the node that follows Schedule 1. This difference in probability increases as the node following Schedule 2 moves closer to the destination. On the other hand, the probability gap diminishes, when both the nodes becomes closer to each other. In addition, because of the distortion by random channels, Schedules 3 and 4, which are in fact not part of the source-destination route, are detected at the destination, showing the same probabilities of false alarm.

Figure 9 shows the combined outage probability of Schedules 1 and 2 against varying values of threshold τ for different transmit power P of the OFDM packet. The curves in Figure 9 indicate that as the value of threshold increases, the outage probability also goes up. This is because, for higher τ, the probability of detecting the energy in a packet decreases.

Lastly, we show the scalability of our proposed model for higher number of hops and a large number of intersecting schedules. It can be seen from Figure 10 that the simulation results are in complete agreement with the analytical results when there are 8 intersecting routes between a source

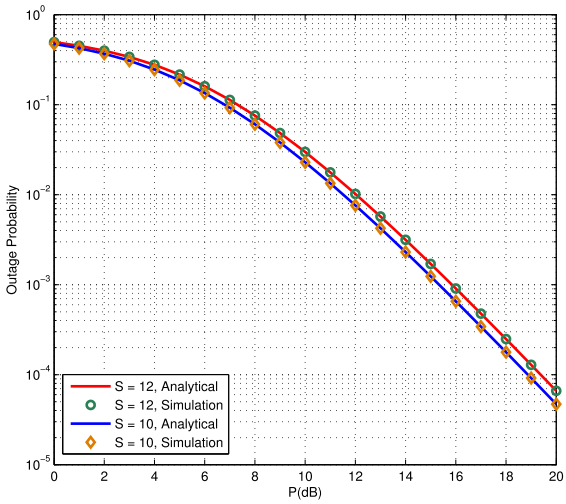

FIGURE 10. The probability of outage versus power with 8 intersecting routes, $K = 3$ and $\tau = 0.5$.

destination pair where each intersecting route appears after 10 hops, i.e., $n_1 = n_2 = \ldots = n_8 = 10$.

VII. CONCLUSION

In this paper, we have proposed a novel physical layer scheduling method to handle multiple flows in large-scale cooperative networks. In the proposed scheme, an OFDM packet for the route set-up is updated to identify the duty cycle schedules in use, as it travels from the source to the destination. The intermediate nodes perform energy detection and insert the information of their own schedule, that they follow, in their respective sub-carriers. When the OFDM packet reaches the destination, the destination detects the occupied schedules and then notify the source of a different schedule available for data transmission through a route reply. We have considered three different detection approaches to process the observations with multiple sub-carriers. The probabilities of detection have been derived for each approach using the Markov chain model for the irreducible state space in discrete time. Furthermore, through numerical and simulation results, we have investigated the impacts of various system parameters such as transmit power P, number of schedules S, number of sub-carriers K, and detection threshold τ.

Considering the fact that high-layer protocols need to be designed for OLA-based networks to fully utilize the gains in the physical layer, our study in this paper can provide important design insights on in the network or system-level optimization. For example, based on the aforementioned analysis and simulation results regarding the outage rate and the false-alarm probability, we can adaptively change the detection method, the transmit power P, the number of schedules S, and the number of sub-carriers per one schedule K, depending on traffic load, node density, power budget of nodes, and quality-of-service (QoS) requirements. Moreover, the analytical model in this paper can be reflected as a module to better characterize the OLA-based routes in network simulators such as NS-3. Future extensions will include

random node placement according to Poisson point process and the framework to maximize the detection probability for a given false-alarm probability threshold.

REFERENCES

[1] J. Huang, Z. Chang, C. Wang, Y. Qian, H. Gharavi, and Z. Li, "Enabling technologies for smart Internet of Things," *IEEE Commun. Mag.*, vol. 56, no. 9, pp. 12–13, Sep. 2018.

[2] T. Qiu, N. Chen, K. Li, M. Atiquzzaman, and W. Zhao, "How can heterogeneous Internet of Things build our future: A survey," *IEEE Commun. Surveys Tuts.*, vol. 20, no. 3, pp. 2011–2027, 3rd Quart., 2018.

[3] R. Singh, B. K. Rai, and S. K. Bose, "Modeling and performance analysis for pipelined-forwarding MAC protocols for linear wireless sensor networks," *IEEE Sensors J.*, vol. 19, no. 15, pp. 6539–6552, Aug. 2019.

[4] H. Jhajj, R. Datla, and N. Wang, "Design and implementation of an efficient multipath AODV routing algorithm for MANETs," in *Proc. IEEE 9th Annu. Comput. Commun. Workshop Conf. (CCWC)*, Jan. 2019, pp. 527–531.

[5] M. Z. Alam, I. Adhicandra, and A. Jamalipour, "Optimal best path selection algorithm for cluster based multi-hop MIMO cooperative transmission for vehicular communications," *IEEE Trans. Veh. Technol.*, to be published. [Online]. Available: https://ieeexplore.ieee.org/abstract/document/8718366

[6] Y. Peng, J. Li, S. Park, K. Zhu, M. M. Hassan, and A. Alsanad, "Energy-efficient cooperative transmission for intelligent transportation systems," *Future Gener. Comput. Syst.*, vol. 94, no. 15, pp. 634–640, May 2019.

[7] N. T. Tuan, D.-S. Kim, and J.-M. Lee, "On the performance of cooperative transmission schemes in industrial wireless sensor networks," *IEEE Trans. Ind. Informat.*, vol. 14, no. 9, pp. 4007–4018, Sep. 2018.

[8] S. A. Hassan, S. S. Syed, and F. Hussain, "Communication technologies in IoT networks," in *Internet of Things: Building Blocks and Business Models* (SpringerBriefs in Electrical and Computer Engineering). New York, NY, USA: 2017, pp. 13–26.

[9] H. K. Narsani, S. A. Hassan, and S. Saleem, "An energy-efficient approach for large scale opportunistic networks," in *Proc. IEEE 88th Veh. Technol. Conf. (VTC-Fall)*, Aug. 2018, pp. 1–5.

[10] J. Lin, H. Jung, Y. J. Chang, J. W. Jung, and M. A. Weitnauer, "On cooperative transmission range extension in multi-hop wireless ad-hoc and sensor networks: A review," *Ad Hoc Netw.*, vol. 29, pp. 117–134, Jun. 2015.

[11] J. Lin and M. A. Weitnauer, "Range extension cooperative MAC to attack energy hole in duty-cycled multi-hop WSNs," *Wireless Netw.*, vol. 24, no. 5, pp. 1419–1437, Jul. 2018.

[12] Q. Wu, X. Zhou, and F. Ge, "A cross-layer protocol for exploiting cooperative diversity in multi-hop wireless ad hoc networks," *Wireless Netw.*, vol. 23, no. 5, pp. 1591–1610, Jul. 2017.

[13] H. Jung and M. A. Weitnauer, "Multi-packet opportunistic large array transmission on strip-shaped cooperative routes or networks," *IEEE Trans. Wireless Commun.*, vol. 13, no. 1, pp. 144–158, Jan. 2014.

[14] K. Shim, T. N. Do, and B. An, "A physical layer security-based routing protocol in mobile ad-hoc wireless networks," in *Proc. 20th Int. Conf. Adv. Commun. Technol. (ICACT)*, Feb. 2018, pp. 417–422.

[15] H. Lim and D. Yoon, "Refinements of binary integration for Swerling target fluctuations," *IEEE Trans. Aerosp. Electron. Syst.*, vol. 55, no. 2, pp. 1032–1036, Apr. 2019.

[16] D. A. Abraham, "Optimization of M-of-N detectors in heavy-tailed noise," in *Proc. MTS/IEEE Charleston OCEANS*, Oct. 2018, pp. 1–10.

[17] A. Akanser, "Energy-efficient reading of correlated wireless sensors," Ph.D. dissertation, School Elect. Comput. Eng., Georgia Inst. Technol., Atlanta, GA, USA, May 2016.

[18] S. Marano, V. Matta, T. He, and L. Tong, "The embedding capacity of information flows under renewal traffic," *IEEE Trans. Inf. Theory*, vol. 59, no. 3, pp. 1724–1739, Mar. 2013.

[19] V. Matta and A. H. Sayed, "Consistent tomography under partial observations over adaptive networks," *IEEE Trans. Inf. Theory*, vol. 65, no. 1, pp. 622–646, Jan. 2019.

[20] X. Jin, A. Saifullah, C. Lu, and P. Zeng, "Real-time scheduling for event-triggered and time-triggered flows in industrial wireless sensor-actuator networks," in *Proc. IEEE Conf. Comput. Commun. (INFOCOM)*, Apr./May 2019, pp. 1684–1692.

[21] A. Adulyasas, Z. Sun, and N. Wang, "Connected coverage optimization for sensor scheduling in wireless sensor networks," *IEEE Sensors J.*, vol. 15, no. 7, pp. 3877–3892, Jul. 2015.

[22] D. Enqing, Q. Fulong, W. Jiaren, Z. Zongjun, Z. Dejing, and S. Huakui, "An energy efficient distributed link scheduling protocol for wireless sensor networks," in *Proc. IEEE 28th Conv. Elect. Electron. Eng. Isr. (IEEEI)*, Dec. 2014, pp. 1–4.

[23] S. Cerovic, R. Visoz, L. Madier, and A. O. Berthet, "Centralized scheduling strategies for cooperative HARQ retransmissions in multi-source multi-relay wireless networks," in *Proc. IEEE Int. Conf. Commun. (ICC)*, May 2018, pp. 1–6.

[24] E. Ahmed, I. Yaqoob, A. Gani, M. Imran, and M. Guizani, "Internet-of-Things-based smart environments: State of the art, taxonomy, and open research challenges," *IEEE Wireless Commun.*, vol. 23, no. 5, pp. 10–16, Oct. 2016.

[25] R. C. Qiu, H. Liu, and X. Shen, "Ultra-wideband for multiple access communications," *IEEE Commun. Mag.*, vol. 43, no. 2, pp. 80–87, Feb. 2005.

[26] E. Seneta, *Non-Negative Matrices and Markov Chains*, 2nd ed. New York, NY, USA: Springer, 2006.

[27] S. M. Ross, *Introduction to Probability Models*, 9th ed. New York, NY, USA: Academic, 2007.

FARHAN NAWAZ received the B.S. degree from the University of Engineering and Technology, Peshawar, Pakistan, in 2016, and the M.S. degree from the National University of Sciences and Technology, Islamabad, Pakistan, in 2018, both in electrical engineering. His research interests include wireless communications, digital signal processing, signals and systems, machine learning, and communications theory.

SYED ALI HASSAN (S'07–M'12–SM'17) received the B.E. degree (Hons.) in electrical engineering from the National University of Sciences and Technology (NUST), Islamabad, Pakistan, in 2004, the M.S. degree in electrical engineering from the University of Stuttgart, Stuttgart, Germany, in 2007, and the M.S. degree in mathematics and the Ph.D. degree in electrical engineering from the Georgia Institute of Technology, Atlanta, GA, USA, in 2011.

He was a Visiting Professor with Georgia Tech, in 2017. He is currently an Associate Professor with the School of Electrical Engineering and Computer Science, NUST, where he is also the Director of the Information Processing and Transmission Research Group, which focuses on various aspects of theoretical communications. His research interest includes signal processing for communications.

ALI JAVED HASHMI received the B.E. degree in avionics engineering from the National University of Sciences and Technology, in 1996, and the Ph.D. degree in electrical engineering from the School of Electrical and Computer Engineering, Georgia Institute of Technology, Atlanta, in 2009. His research interests include deep space optical communication, adaptive optics, and hybrid communication systems.

HAEJOON JUNG received the B.S. degree (Hons.) from Yonsei University, South Korea, in 2008, and the M.S. and Ph.D. degrees from the Georgia Institute of Technology (Georgia Tech), Atlanta, GA, USA, in 2010 and 2014, respectively, all in electrical engineering. From 2014 to 2016, he was a Wireless Systems Engineer at Apple, Cupertino, CA, USA. Since 2016, he has been an Assistant Professor with Incheon National University, Incheon, South Korea. His research interests include communication theory, wireless communications, wireless power transfer, and statistical signal processing.